DOI 10.1007/s11595-017-1682-y

Effect of Strontium Substitution on Microstructure and Magnetic Properties of Electrospinning $BaFe_{12}O_{19}$ Nanofibers

HOU Chuanxin[1], LIU Guifang[1], DANG Feng[1*], ZHANG Zidong[1], CHEN Ju[2]

(1. Key Laboratory for Liquid-Solid Structural Evolution & Processing of Materials Ministry of Education, Shandong University, Jinan 250061, China; 2. Shandong Chunxu Chemical Design Co., Ltd., Jinan 250061, China)

Abstract: Barium ferrite micro/nano fibers were successfully prepared via the electrostatic spinning by using dimethyl formamide (DMF) as the solvent, and poly vinyl pyrrolidone (PVP) as the spinning auxiliaries. Effects of strontium substitution on the structure, morphology, and magnetic properties were investigated by scanning electron microscope (SEM), X-ray diffraction analysis (XRD), and vibration sample magnetometer (VSM). XRD patterns of the samples confirm that pure barium ferrite fibers form, and the Sr substitution makes the main peaks (110), (107), and (114) move to right slightly. Also, the FE-SEM images show that the Sr substituted fibers can keep complete fibrous morphology. Moreover, the VSM results demonstrate that the saturation magnetization can reach 56.7 emu/g when the fibers are calcined at 800℃.

Key words: electrostatic spinning; Sr substituted barium ferrite fibers; magnetic properties

Introduction

Nanofibers are One-dimensional nanomaterials, including nanotubes, nanowires, nanoribbons, nanorods, *etc*[1]. Due to the high length-diameter ratio and anisotropy characteristics, nanofibers have many special properties, such as thermal properties, optical properties, electrical properties, magnetic properties, chemical properties and some other properties. As a result, one-dimensional nanomaterials have drawn more attention in the field of nanometer materials by scientists in recent years[2].

The magnetic properties of materials have been studied for many years[3-7]. It is widely accepted that two categories of ferrites, hard ferrites with high coercivity and soft ferrites with low coercivity presented in front of us. $BaFe_{12}O_{19}$ is a kind of hard magnetic material of M-type hexaferrites, which has been widely used in lots of technological applications, such as permanent magnets, microwave devices, magneto-optics, magnetic recording medium sensors and some other aspects, due to their excellent chemical stability and high uniaxial magnetic crystalline anisotropy. However, the high specific gravity of single-phase, just like microwave absorbing and shielding materials has limited its applications in many fields. With the development of modern science and technology, all kinds of electronic and electrical devices have become an indispensable part of people's daily life and social development. At the same time, the electromagnetic radiation and interference caused by these devices during work process also lead to the increasing deterioration of people's living space, and not only affect communication, but also pose a threat to human health. Electromagnetic shielding is one of the main means to restrain electromagnetic interference and realize the protection of electromagnetic radiation[8]. Owing to the distinctive crystal structure, barium ferrites have high saturation magnetization, excellent chemical stability, high coercive force, and large uniaxial magnetic anisotropy. Furthermore, the production of low cost barium ferrites makes it play an important role in the production of hard magnetic materials, electromagnetic shielding magnetic, recording media and microwave devices[9-11]. Up to now, there have been a vast number of researches on barium ferrites, especially the one-dimensional nanomaterials of barium ferrites in virtue of their potential applications[12].

(Received: Oct. 20, 2016; Accepted: Dec. 9, 2016)

HOU Chuanxin(侯传信): E-mail: 15275319606@163.com

*Corresponding author: DANG Feng(党锋): Ph D; Prof.; E-mail: dangfeng@sdu.edu.cn

Funded by the Qilu Program in Shandong University and the Natural Science Foundation of Shandong Province (ZR2014EMM001)

The performance of barium ferrites depends strongly on their structure, chemistry, morphology and doping elements, which often result from the methods of synthesis. Until now, a great deal of work has been done to investigate its properties by changing the methods of preparation of the one-dimensional nanomaterials of barium ferrites (such as solid-state reaction, sol-gel method, molten-salt synthesis, solvothermal, and electrospinning[13,14]), chemical composition, doping elements, sintering temperature, time, *etc*[15-17]. Among all the synthetic methods, electrostatic spinning has attracted great enthusiasm for the researcheres and scientists because this method is not only simple to handle, easy to regulate the operating parameters, but also can be used to obtain well-proportioned sized nanofibers with the submicron range consistently and produce all kinds of fibers of materials, including organic materials, inorganic materials, metals, composites, *etc*[18,19]. which are difficult to obtained by other methods. Meanwhile, with the development of electrospinning technology, it has become one of the most indispensable methods for the preparation of inorganic materials nowadays[20-22], just like Ag-ZnO, TiO_2, NiO-SnO_2 and $BaFe_{12}O_{19}$.

Several kinds of factors will influence the morphology, phase composition and properties of the $BaFe_{12}O_{19}$, such as the solvent, dopings, temperature, electrospinning parameters, and the content of PVP. In this work, barium ferrites were obtained by adding Sr[23] element aiming to research the effect of Sr element on the properties of $BaFe_{12}O_{19}$ by a combined technique of electrostatic spinning and high-temperature heating treatment. The results showed that the Sr substituted fibers ($BaSrFe_{12}O_{19}$) can keep complete fibrous morphology and enhance the the saturation magnetization of pure $BaFe_{12}O_{19}$.

2 Experimental

A certain amount (a molar ratio of Fe/Ba was 11.5:1) of barium nitrate [$Ba(NO_3)_2$, AR], ferric nitrate [$Fe(NO_3)_3]\cdot 9H_2O$, AR] and strontium nitrate [$Sr(NO_3)_2$, AR] were dissolved in 20.0 mL dimethyl formamide (DMF). After they were dissolved completely, moderate amount of PVP was added and then stirred until a homogeneous transparent brown solution formed. The precursor solution was prepared and set for a few hours in order to eliminate air bubbles.

In a typical electrospinning process, the spinneret containing the precursor solution had an inner diameter of about 1 mm. A distance of 15 cm and voltage of 13 kV were maintained between the tip of the spinneret and the collector. After completing to collect precursor fibers, they were dried in a drying oven in air atmosphere at 80℃ firstly and then calcined at 800 ℃ for 2 h in a muffle furnace to obtain the $BaFe_{12}O_{19}$ and $BaSrFe_{12}O_{19}$ fibers[24].

The phase compositions of barium ferrites were investigated by X-ray diffraction (XRD, XD-3, China) with Cu Kα (λ=1.540 Å) radiation over Bragg angle ranging from 10 to 90°. The SEM images of barium ferrites were investigated by a scanning electron microscope (SEM). The magnetic hysteresis loops of the magnets were measured using a vibrating sample magnetometer (VSM, HH-15) in applied maximum magnetic field up to 1.2 T[25] at room temperature.

3 Results and discussion

Fig.1 shows the X-ray diffraction patterns of Sr substituted barium ferrite fibers calcined at different tempreture. Combined with our previous work, pure barium ferrite fibers are achieved after calcined at different tempreture of 800, 900, and 1 000 ℃, respectively. And Sr substitution makes the main peaks (110), (107), and (114) move to right slightly because positions of the barium elements were occupied by strontium elements partly[23]. All the strong diffraction peaks of samples can be perfectly indexed as the magneto-plumbite structure for $BaFe_{12}O_{19}$. No other characteristic peaks for impurity are observed. But the diffraction peaks of samples calcined at 900 ℃ and 1 000 ℃ are stronger than samples calcined at 800 ℃. It is proved that when the calcination temperature increases, the crystallinity of the sample increases.

SEM images of the Sr substituted barium ferrite

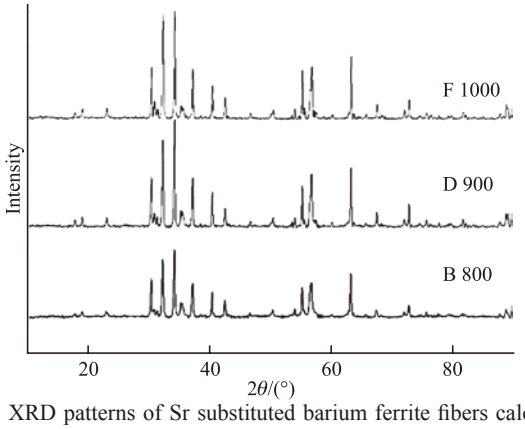

Fig.1 XRD patterns of Sr substituted barium ferrite fibers calcined at different temperatures

precursor fibers (a, b) and Sr substituted barium ferrite fibers calcined at different temperatures are shown in Fig.2. Meanwhile, it must be pointed out that different morphology (Figs.2(a) and 2(b)) can be obtained by the same solution under different environmental conditions. Due to the high concentration of PVP, the solvent evaporates slowly, coupled with the impact of environmental conditions. With the same spinning solution, fibers with different morphology were obtained. As can be seen from image (a), the diameter of precursor fibers is around 0.6 μm. The morphology of ferrite looks like ribbons as shown in Fig.2(b) and the diameter of precursor is around 6 μm. After the precursor fibers were calcined at 800, 900, and 1000 ℃, respectively, the fibers remain intact basically. At the same time, it is indicated that the fibers are indeed composited of particles of different sizes which are interrelated. In the flowing heat treatment processes, PVP and the remainder solvents were all evaporated and the inorganic salt crystallized. All of these lead to the rough surfaces that can be seen from Fig.2[26,27].

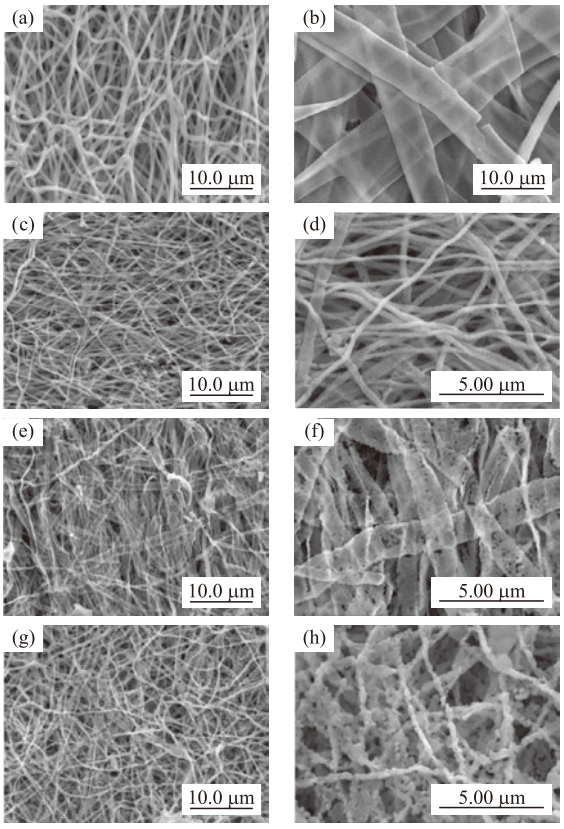

Fig.2 SEM images of $BaSrFe_{12}O_{19}$ ferrites: (a, b) precursor fibers; (c, d) fibers calcined at 800 ℃; (e, f) fibers calcined at 900 ℃; (g, h) fibers calcined at 1 000℃

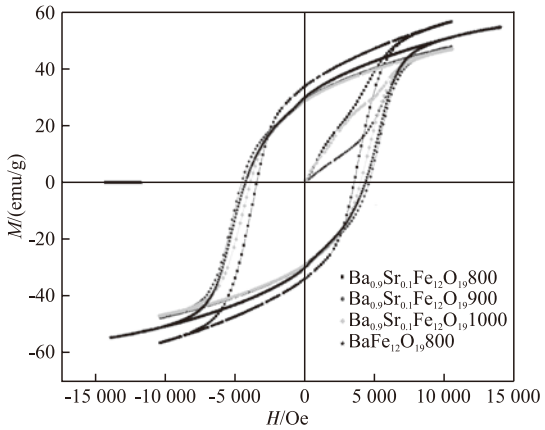

Fig.3 Hysteresis loops of Sr substituted barium ferrite fibers measured at room temperature

Table 1 Value of magnetic properties of the sample 1

Sample	Calcinate temperature/℃	M_s /(emu/g)	M_r /(emu/g)	H_c /(Oe)	M_r/M_s
$BaFe_{12}O_{19}$	800	54.69	29.99	4300	0.548
$BaSrFe_{12}O_{19}$	800	56.70	33.79	3463	0.596
$BaSrFe_{12}O_{19}$	900	47.60	28.79	4529	0.605
$BaSrFe_{12}O_{19}$	1000	46.80	28.79	3962	0.615

VSM technique was used to explore the dynamical magnetic properties of the Sr substituted barium ferrite fibers. The hysteresis loops were measured to determine the magnetic parameters such as the specific saturation magnetization (M_s), remanent magnetization (M_r) and coercivity (H_c). Fig.3 shows representative hysteresis curves of the Sr substituted barium ferrite fibers calcined at 800 ℃ measured at room temperature. And the detailed M_s, M_r, H_c/Oe and M_r/M_s values of the ferrite fibers calcined at different temperature are shown in Table 1. It can be seen from Fig.3 that the saturation magnetization of the sample calcined at 800 ℃ is the highest. Because the morphology of the sample calcined at 800 ℃ is banded the grain size of $BaSrFe_{12}O_{19}$ is smaller than 100 nm. As can be seen from Table 1, the saturation magnetization of Sr substituted barium ferrite fibers decreases with increasing temperature. The coercive force increases firstly, and then decreases with the increasing temperature. The value of M_r/M_s increases with doping Sr compared with pure $BaFe_{12}O_{19}$, and increases with increasing calcined temperature. When the calcined teperature is 800℃, the Sr substituted barium ferrite fibers have small grain size which has resulted in the higher saturation magnetization and lower coercivity.

4 Conclusions

Sr substituted barium ferrite micro/nano fibers were obtained by the electrostatic spinning method. Compared with pure $BaFe_{12}O_{19}$, the main peaks of

XRD of Sr substituted barium ferrite micro/nano fibers move to right slightly due to the positions of barium elements occupied by doping Sr elements partly. The Sr substituted fibers can keep complete fibrous morphology. When the calcined teperature is 800 ℃, the Sr substituted barium ferrite fibers have small grain size which has resulted in the higher saturation magnetization and lower coercivity. The VSM results demonstrated that the saturation magnetization can reach 56.7 emu/g and the coercivity can reduce to 3463 Oe.

References

[1] Zhang ZK, Cui ZL. *Nanomaterials and Nanotechnology*[M]. 2000, 1-126

[2] Dai JF, Dai YL, Wang ZX, *et al*. Preparation and Magnetic Properties of Lanthanum-and Cobalt-codoped M-type Strontium Ferrite Nanofibres[J]. *Journal of Experimental Nanoscience,* 2013 (ahead-of-print): 1-9

[3] Shi ZC, Fan RH, Yan KL, *et al*. Preparation of Iron Networks Hosted in Porous Alumina with Tunable Negative Permittivity and Permeability[J]. *Advanced Functional Materials,* 2013, 23(23): 4 123-4 132

[4] Shi ZC, Chen SG, Sun K, *et al*. Tunable Radio-frequency Negative Permittivity in Nickel-alumina "Natural" Meta-composites[J]. *Applied Physics Letters,* 2014, 104(25): 252 908-252 908-5

[5] Yan KL, Fan RH, Shi ZC, *et al*. Negative Permittivity Behavior and Magnetic Performance of Perovskite La1-xSrxMnO$_3$ at High-frequency[J]. *Journal of Materials Chemistry C,* 2014, 2(6): 1 028-1 033

[6] Wang XA, Shi ZC, ChenM, *et al*. Tunable Electromagnetic Properties in Co/Al$_2$O$_3$ Cermets Prepared by Wet Chemical Method[J]. *Journal of the American Ceramic Society,* 2014, 97(10): 3 223-3 229

[7] Qian L, Lu L, Fan RH. Tunable Negative Permittivity Based on Phenolic Resin and Multi-walled Carbon Nanotubes[J]. *Rsc Advances,* 2015, 5(22): 16 618-16 621

[8] Kosanda DE. *Electromagnetic Signal Interference Shielding Gasket Apparatus*[P]. US Patent 4, 762, 966: 1988, 8-9

[9] Radwan M, Rashad M, Hessien M. Synthesis and Characterization of Barium Hexaferrite Nanoparticles[J]. *Journal of Materials Processing Technology, 2007,* 181 (1): 106-109

[10] Pullar RC. Hexagonal Ferrites: Are View of the Synthesis, Properties and Applications of Hexaferrite Ceramics[J]. *Progress in Materials Science,* 2012,57 (7) : 1 191-1 334

[11] Mosleh Z, Kamelin P, Ranjbar M, *et al*. Effect of Annealing Temperature on Structural and Magnetic Properties of BaFe$_{12}$O$_{19}$ Hexaferrite Nanoparticles[J]. *Ceramics International,* 2014, 40: 7 279-7 284

[12] Dai J, Dai Y, Wang Z. Preparation and Magnetic Properties of Lanthanum-and Cobalt-codoped M-type Strontium Ferrite Nanofibres[J]. *Journal of Experimental Nanoscience* (ahead-of-print), 2013: 1-9

[13] Chen D, Qiao X, Qiu X, *et al*. Convenient Synthesis of Silver Nanowires with Adjustable Diameters via a Solvothermal Method[J]. *Journal of Colloid and Interface Science,* 2010; 344: 286-291

[14] Shen X, Liu M, Song F, *et al*. Structural Evolution and Magnetic Properties of SrFe$_{12}$O$_{19}$ Nanofibers by Electrospinning[J]. *Journal of Sol-gel Science and Technology,* 2010, 53: 448-453

[15] Xu P, Han X, Jiang J, *et al*. Synthesis and Characterization of Novel Coralloid Polyaniline/BaFe$_{12}$O$_{19}$ Nanocomposites[J]. *Journal of Physical Chemistry C,* 2007, 111(34): 12 603-12 608

[16] Li Z W, Wu Y P, Lin G Q, *et al*. Static and Dynamic Magnetic Properties of CoZn Substituted Z-type Barium Ferrite Ba$_3$Co$_x$Zn$_2$-*x*Fe$_{24}$O$_{41}$ Composites[J]. *Journal of Magnetism & Magnetic Materials*, 2007, 310: 145-151

[17] Temuujin J, Aoyama M, Senna M, *et al*. Preparation and Properties of Ferromagnetic Z-type Hexaferrite from Wet Milled Mixtures of Intermediates[J]. *Journal of Magnetism & Magnetic Materials*, 2007, 311(2): 724-731

[18] Li CJ, Huang BN, Wang JN. Effect of Aluminum Substitution on Microstructure and Magnetic Properties of Electrospun BaFe$_{12}$O$_{19}$ Nanofibers[J]. *Journal of Materials Science*, 2013, 48(4) : 1 702-1 710

[19] Joo J, Park KT, Kim BH, *et al*. Conducting Polymer Nanotube and Nanowire Synthesized by Using Nanoporous Template: Synthesis, Characteristics, and Applications[J]. *Synthetic Metals*, 2003, 135(135): 7-9

[20] Yu HQ, Song HW, Pan GH. Preparation and Luminescent Properties of YVO$_4$: Eu^{3+} Nanofibers by Electrospinning[J]. *Journal of Nanoscience and Nanotechnology,* 2008, 8(3): 1 432-1 436

[21] Zhang SH, Dong XT, Xu SZ. Preparation and Characteristic of TiO$_2$@SiO$_2$ Submicron Coaxial Cable[J]. *Journal of Materials Chemistry,* 2007,65 (23): 2 675-2 679

[22] Dong XT, Wang JX, Cui QZ. Preparation of LaFeO$_3$ Porous Hollow Nanofibers by Electrospinning[J]. *International Journal of Chemistry,* 2009, 1(1): 13-17

[23] Yan KL, Fan RH, Chen M, *et al*. Perovskite (La,Sr)MnO$_3$ with Tunable Electrical Properties by the Sr-doping Effect[J]. *Journal of Alloys & Compounds,* 2015, 628: 429-432

[24] Fan LJ, Dong XT, Gao XB, *et al*. Synthesis and Characterization of BaFe$_{12}$O$_{19}$ Nanofibres Via an Electrospinning Technique[J]. *Acta Armamentarii*, 2011, 32(1): 112-117

[25] Huang BN, Li CJ, Wang JN. Template Synthesis and Magnetic Properties of Highly Aligned Barium Hex a Ferrite (BaFe$_{12}$O$_{19}$) Nanofibers[J]. *Journal of Magnetism & Magnetic Materials*, 2013, 335:28-31

[26] Wang ZJ, Li ZY, Sun JH, *et al*. Improved Hydrogen Monitoring Properties Based on P-NiO/n-SnO$_2$ Heterojunction Composite Nanofibers[J]. *The Journal of Physical Chemistry C*, 2010,114: 6 100-6 105

[27] Song FZ, Shen XQ, Xiang J, *et al*. Characterization and Magnetic Properties of Ba$_x$Sr$_{1-x}$Fe$_{12}$O$_{19}$ (*x*=0-1) Ferrite Hollow Fibers via Gel-precursor Transformation Process[J]. *Journal of Alloys & Compounds*, 2010, 507: 297-30